FIRST RESULTS OF A LONGITUDINAL PHASE SPACE TOMOGRAPHY AT PITZ

D. Malyutin*, M. Gross, I. Isaev, M. Khojoyan, G. Kourkafas, M. Krasilnikov, B. Marchetti, F. Stephan, G. Vashchenko, DESY, 15738 Zeuthen, Germany

Abstract

The Photo Injector Test facility at DESY, Zeuthen Site (PITZ), was established as a test stand of the electron source for FLASH and the European X-ray Free Electron Laser (XFEL). One of the tasks at PITZ is the detailed characterization of longitudinal properties of the produced electron bunches.

The measurements of the electron bunch longitudinal phase space can be done by tomographic methods using measurements of the momentum spectra by varying the electron bunch energy chirp. At PITZ the energy chirp of the electron bunch can be changed by varying the RF phase of the accelerating structure downstream the gun. The resulting momentum distribution can be measured in a dispersive section installed downstream the accelerating structure.

The idea of the measurement and the tomographic reconstruction technique is described in this paper. The setup and first measurement results of the bunch longitudinal phase space measurements using the tomographic technique for several electron bunch charges, including 20 pC, 100 pC and 1 nC, are presented as well.

INTRODUCTION

High brilliance photon sources like high gain Free Electron Lasers (FELs) have strong requirements on the electron beam quality used for the production of photon beam. This implies: small transverse beam emittance, high peak current and small energy spread [1]. To satisfy these requirements the electron bunch must be well prepared already in the injector part of the accelerator, i.e. at the electron source.

The Photo Injector Test facility at DESY, Zeuthen Site (PITZ) was built as a test stand for the electron source for FLASH and the European XFEL [2]. A normal conducting L-band 1.6-cell copper gun cavity with a Cs_2Te photocathode generates about 7 MeV electron bunches with ~20 ps bunch length FWHM and up to several nC charge. Then the electrons are further accelerated by an accelerating structure to an energy of up to about 27 MeV. Downstream the accelerating structure the PITZ beamline consists of various diagnostic devices for detailed measurements of the electron beam properties. Characterization of the electron bunch transverse phase space at PITZ is mainly done by a slit scan technique [3]. For electron bunch length measurements and longitudinal phase space measurements a streak camera system was used in the last years in the straight section and in dispersive sections, respectively [4]. A recently installed RF deflector is expected to provide a much better time resolution and new possibilities to study the bunch longitudinal properties compared to the streak camera [5] in the near future. Besides the measurements with the RF deflector or with the streak camera, the electron bunch longitudinal phase space can also be measured using a tomographic technique [6]. Measuring the momentum distribution for different RF phases of the accelerating structure, the longitudinal phase space can be restored applying tomographic reconstruction to the measured distributions. From the restored phase space the slice energy spread, the time-energy correlation and the beam current distribution can be extracted. In contrary to a measurement with the RF deflector, this method is a multi-shot technique as the set of momentum distributions cannot be measured at once.

The current PITZ beamline schematic layout is shown in Fig. 1. The main components of the PITZ setup are a photocathode laser system, an RF photo-electron gun surrounded by a main and a bucking solenoid, an accelerating structure – cut disk structure (CDS) which is also called booster cavity, three dipole spectrometers – one in the low energy section downstream the gun (Low Energy Dispersive Arm – LEDA), a second one in the high energy section downstream the booster (the first High Energy Dispersive Arm – HEDA1) and a third one in the end of the PITZ beamline (the second High Energy Dispersive Arm – HEDA2), three Emittance Measurement Stations (EMSYs), a transverse deflecting structure (TDS) and a phase space tomography module (PST).

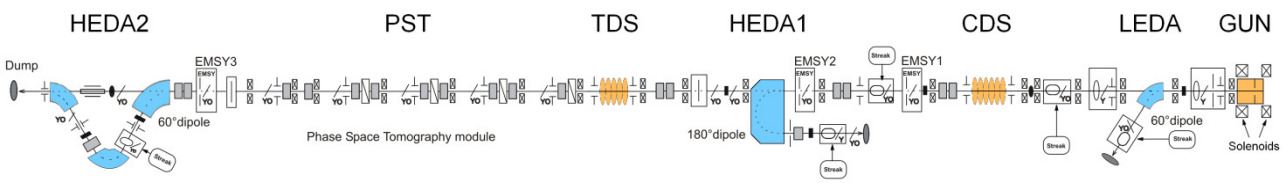

Figure 1: PITZ beamline schematic layout. The beam propagates from right to left.

*dmitriy.malyutin@desy.de

ISBN 978-3-95450-126-7

Several diagnostics components between the gun and the booster are used for the low energy electron bunch characterization: two faraday cups (FCs) and one integrating current transformer (ICT) for bunch charge measurements and three screen stations for beam position and beam size measurements. Downstream the booster cavity the beamline consists of different types of diagnostic devices for detailed high energy electron bunch characterization. There are several ICTs for bunch charge measurements. Three dedicated screen stations can be used for beam position and beam size measurements as well as for transverse emittance measurements utilizing the slit scan technique [3]. A phase space tomography module located further downstream can also be used for transverse phase space measurements and can simultaneously restore the horizontal and the vertical transverse planes [7].

LONGITUDINAL PHASE SPACE TOMOGRAPHY

Tomographic reconstruction techniques can be used for measurements of the longitudinal phase space as the input projections correspond to the momentum spectra where the bunch energy chirp has been varied [6]. After that, the electron bunch longitudinal profile and slice energy spread can be extracted from the reconstructed longitudinal phase space and the longitudinal emittance can be calculated.

At PITZ such measurements can be performed by varying the RF phase of the CDS booster. The momentum spectra downstream the booster measured at the HEDA1 or at the HEDA2 dispersive sections can be used to feed the tomographic reconstruction.

Algebraic Reconstruction Technique

In algebraic reconstruction technique (ART) the 2D object of tomographic reconstruction, represented as one dimensional array g, can be obtained from an iterative procedure (1) over the projections, starting from an initial guess $g^{(0)}$ [8]:

$$g_q^{(k+1)} = g_q^{(k)} + \sum_{i,j} \frac{a_{i,j,q}\left(p_{i,j} - \sum_l a_{i,j,l} \cdot g_l^{(k)}\right)}{\sum_{n,m} a^2_{i,n,m}}, \quad (1)$$

where k is the current iteration number, $p_{i,j}$ are the measured momentum distributions for all booster RF phases i, and j is the bin index of the momentum distribution, $a_{i,j,l}$ is the matrix, which describes the transport function of the booster in terms of particle longitudinal momentum such that:

$$p_{i,j} = \sum_l a_{i,j,l} \cdot g_l \,. \quad (2)$$

Procedure (1) is then iterated until the desired convergence is reached.

Acceleration Model

The matrix $a_{i,j,l}$ for the iterative procedure (1) is generated according to the model which describes particle acceleration. The acceleration of an ultra-relativistic electron bunch in an accelerating structure can be described as [9]:

$$p = p_0 + V \cdot \cos(\varphi), \quad (3)$$

where p_0 is the bunch initial momentum, V is the maximum momentum gain induced by the accelerating structure, φ is the RF phase of the structure relative to the maximum mean momentum gain (MMMG) phase $\varphi = 0$ and p is the bunch final momentum.

The resulting bunch momentum chirp k induced by an accelerating structure can be calculated from Eq. (3) as:

$$k = -\frac{dp}{dt} = V\omega \cdot \sin(\varphi), \quad (4)$$

where $\omega = 2\pi f$ and f is the RF frequency in the structure.

Since the acceleration by the accelerating structure cannot cause full 90° rotation of the longitudinal phase space, the temporal resolution will be limited by the maximum momentum chirp applied to the bunch, the slice momentum spread in the bunch and the momentum resolution of the momentum distribution measurement system.

The time resolution σ_t for the electron bunch slice momentum spread σ_δ can be estimated from the maximum momentum chirp k_{max} applied to the bunch:

$$\sigma_t = \frac{\sigma_\delta}{k_{max}}. \quad (5)$$

Here it is assumed that the resolution of the momentum measurement is much smaller than the bunch slice momentum spread.

MEASUREMENT SETUP

Measurements of the beam momentum distribution at PITZ downstream the CDS booster can be done at two different points of the beamline: at the HEDA1 and at the HEDA2 dispersive sections. Both sections are designed for high resolution momentum measurements for various momentum distributions and charges [10].

The HEDA1 dipole (Disp2.D1) is a 180° sector dipole magnet and deflects the electron beam in vertical direction. The location of this dipole in the PITZ beamline is shown in Fig. 1. A more detailed schematic diagram of the HEDA1 section is shown in Fig. 2.

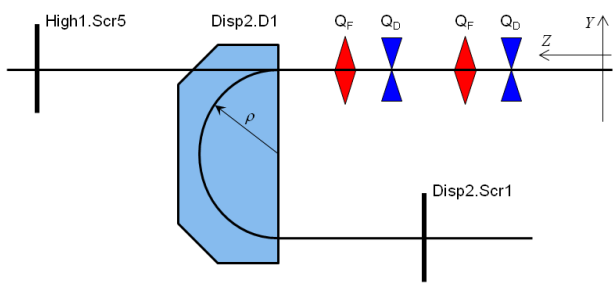

Figure 2: The HEDA1 momentum measurement setup. The beam propagates from right to left.

ISBN 978-3-95450-126-7

The momentum distribution is measured as a vertical profile of the beam on the observation screen Disp2.Scr1. A reference screen – High1.Scr5 and quadrupole magnets upstream the dipole (Q_F and Q_D) are used to optimize the setup for the best momentum resolution [11]. The momentum resolution achieved in the measurements presented in this work was about 5 keV/c for 20 pC and 100 pC bunch charges and about 22 keV/c for 1 nC.

Machine Parameters

A flat-top laser temporal profile with a duration of 17.4 ps FWHM (about 5.2 mm FWHM length or 1.54 mm RMS) was used for the longitudinal phase space measurements. The laser intensity was adjusted to produce bunch charges of 20 pC, 100 pC and 1 nC. The used laser transverse distribution was radially uniform with a diameter of ~1.4 mm.

The RF power in the gun cavity was chosen in such a way that 6.8 MeV/c maximum mean momentum at the gun exit was obtained. That corresponds to about 6.8 MW RF peak power in the gun and 60.5 MV/m maximum electric field at the cathode surface.

The RF power fed to the CDS booster cavity was chosen to have an electron bunch maximum mean momentum at the booster exit of ~22.3 MeV/c. This corresponds to about 3.2 MW RF peak power in the booster and 18 MV/m maximum electric field.

The gun main solenoid current was chosen to deliver good beam transport up to the HEDA2 section without beam losses and good momentum resolution at the HEDA1 and HEDA2 sections.

EXPERIMENTAL RESULTS

Figure 3 shows the measured mean beam momentum and RMS momentum spread of the beam in the HEDA1 section as a function of the booster RF phase, relative to the MMMG phase, for the case of 20 pC bunch charge. The green curve on the upper plot in Fig. 3 shows the predicted bunch mean momentum as a function of the booster RF phase according to Eq. (3). The acceleration model agrees quite well with the measurement data. The momentum deviations in the range from -20° to -10° can be explained by a small temperature drift of the gun or booster cavities during the measurements.

The used booster RF phase range was from -24° to +24° with respect to the MMMG phase and the beam maximum mean momentum gain was V = (22.3 – 6.8) MeV/c = 15.5 MeV/c, where 22.3 MeV/c is the maximum mean momentum downstream the booster and 6.8 MeV/c is the maximum mean momentum downstream the gun. As a result, the maximum momentum chirp k, calculated according to Eq. (4), is 54 keV/c/ps. The resulting temporal resolution σ_t of the reconstructed longitudinal phase space is about 0.2 ps or 60 μm for a slice momentum spread of the bunch σ_δ = 10 keV/c (see Eq. (5)).

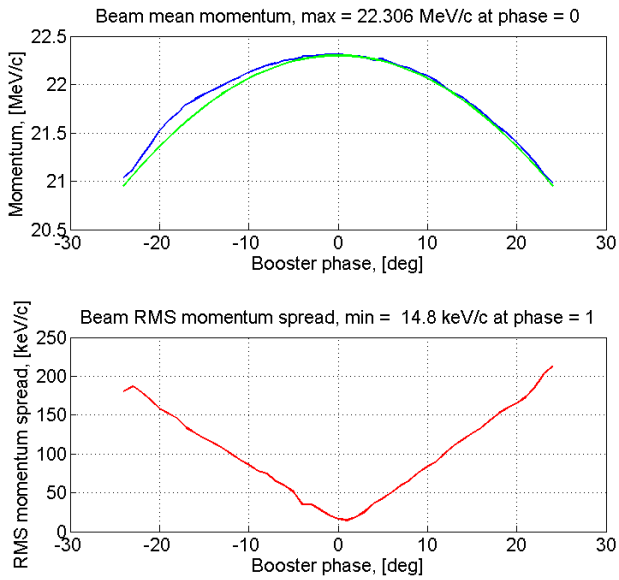

Figure 3: Top: the beam mean momentum as a function of the booster RF phase for 20 pC bunch charge, blue curve: measurement; green: model (3). Bottom: RMS momentum spread, red curve, as a function of the booster RF phase.

The measured bunch momentum distributions for 20 pC bunch charge are shown in Fig. 4 as a 2D histogram for different booster RF phases. Each momentum distribution is plotted relatively to its mean value, and the booster phases are shown relative to the MMMG phase.

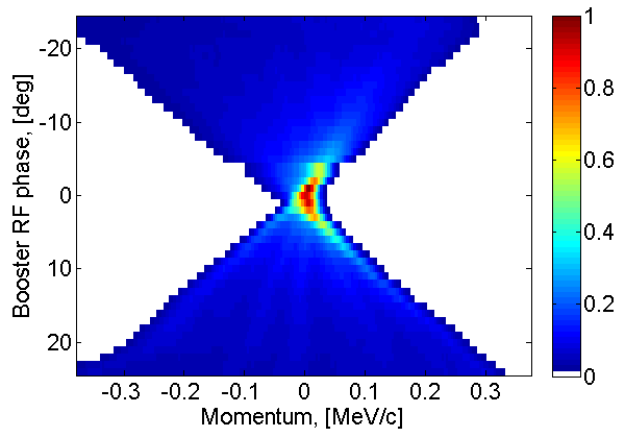

Figure 4: 2D histogram of the bunch momentum distributions plotted in the horizontal lines, for different booster RF phases shown on the vertical axis, for 20 pC bunch charge.

The histogram in Fig. 4 represents the $p_{i,j}$ array used in the reconstruction algorithm Eq. (1,2).

Figure 5 shows the reconstructed longitudinal phase spaces after 100 iterations for the three bunch charges: 20 pC, 100 pC and 1 nC. A 15% charge cut was applied to the phase spaces in order to remove tomographic reconstruction artifacts.

ISBN 978-3-95450-126-7

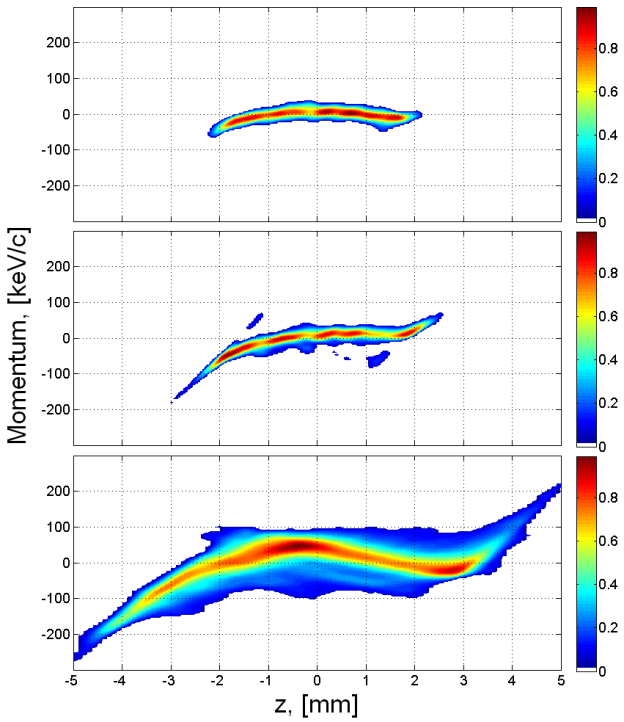

Figure 5: Reconstructed longitudinal phase spaces downstream the booster. The top plot shows the phase space for 20 pC bunch charge, the middle for 100 pC and the bottom for 1 nC. A 15% charge cut is applied.

The calculated RMS bunch length, RMS longitudinal emittance and RMS momentum spread for a 15% charge cut are presented in Table 1.

Table 1: Reconstructed Bunch Parameters

	20 pC	100 pC	1 nC
Bunch length, [mm], σ_z	1.1	1.3	2.2
Emittance, [mm keV/c], ε_z	16.9	25.6	112.9
Momentum spread, [keV/c], δp_z	15.7	30.1	62.6

Figure 6 shows the bunch current profiles, obtained from the reconstructed longitudinal phase spaces, Fig. 5, and the laser temporal profile.

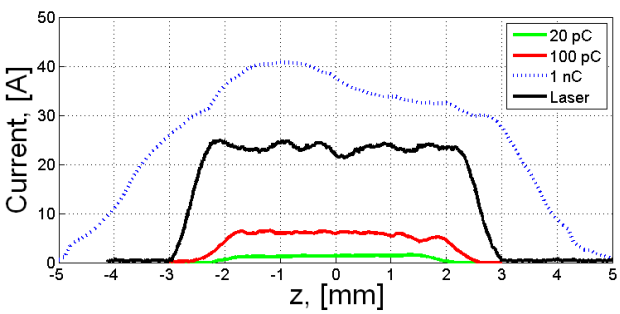

Figure 6: Current profiles of the reconstructions shown in Fig. 5. The green curve is for 20 pC, the red one is for 100 pC and the blue one is for 1 nC bunch charge. The black curve shows the laser temporal profile scaled to the 25 Amps.

Compared to the cathode laser pulse length the electron bunch is longer for 1 nC and is shorter for 100 pC and 20 pC bunch charges. Numerical simulations show the same behavior. Compression for the small charges can be explained by bunch compression during initial acceleration when electrons just started from the cathode surface, since for the MMMG phase of the gun the tail of the bunch sees a higher accelerating field than the head. For high charge the longitudinal space charge forces start to play a significant role and elongate the bunch.

The slice momentum spread calculated for each measured longitudinal phase space with a slice length of 0.3 mm is shown in Fig. 7.

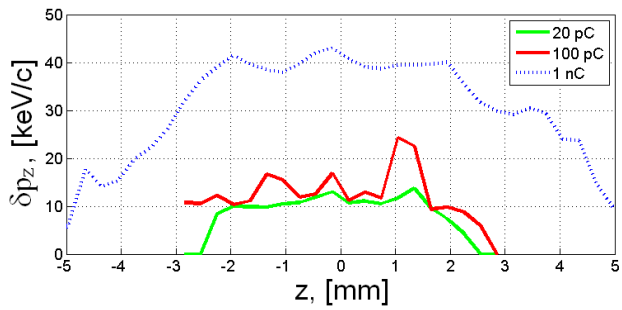

Figure 7: Slice momentum spread calculated from the reconstruction shown in Fig. 5. The green curve is for 20 pC, the red one is for 100 pC and the blue one is for 1 nC bunch charge.

The minimal calculated slice momentum spread of 10 keV/c looks like the systematic limit for such measurements, which arises from the resolution limit in momentum measurements, estimated as 5 keV/c for 20 pC bunch charge. In contrast to the measurements, the numerical simulations of the bunch acceleration by the gun and the booster cavity result in a slice momentum spread less than 1 keV/c.

CONCLUSION

The electron bunch longitudinal phase space was measured at PITZ for different bunch charges using a tomographic technique with ART algorithm. The measured bunch length for 20 pC, 100 pC and 1 nC was compared with the cathode laser pulse duration. The slice momentum spread was calculated. The longitudinal emittance was determined.

The tomographic technique can be used at PITZ as an alternative method for longitudinal phase space measurements while the RF deflector is not available yet.

REFERENCES

[1] P. Schmueser, M. Dohlus, and J. Rossbach, *Ultraviolet and Soft X-Ray Free-Electron Lasers*. (Springer, 2008).

[2] F. Stephan, C. H. Boulware, M. Krasilnikov, J. Bähr et al., "Detailed characterization of electron sources yielding first demonstration of European X-ray Free-Electron Laser beam quality." Phys. Rev. ST Accel. Beams 13, 020704 (2010).

ISBN 978-3-95450-126-7

[3] L. Staykov et al., "Measurement of the projected normalized transverse emittance at PITZ", FEL2007, MOPPH055.
[4] J. Rönsch et al., "First Measurement Results from the Upgraded Low Energy Longitudinal Phase Space Diagnostics at PITZ", FEL2008.
[5] D. Malyutin et al., "Simulation of the longitudinal phase space measurements with the transverse deflecting structure at PITZ", IPAC2012, MOPPP034.
[6] H. Loos et al., "Longitudinal phase space tomography at the SLAC Gun Test Facility and the BNL DUV-FEL", Nucl. Instrum. Meth. A 528 (2004) 189.
[7] G. Asova et al., "Implementation of tomographic diagnostics at PITZ", DITANET2011.
[8] A.C. Kak, M. Slaney, *Principles of Computerized Tomographic Imaging*, (IEEE Press, 1979).
[9] J. Le Duff, "*Dynamics and acceleration in linear structures*", CERN Accelerator School, Fifth General Accelerator Physics Course, Jyväskylä, Finland, 7–18 September 1992, CERN 94-01.
[10] S. Rimjaem et al., "Physics and technical design for the second high energy dispersive section at PITZ", DIPAC2009, MOPD26.
[11] J. Rönsch et al., "First measurements of the longitudinal phase space distribution using the new high energy dispersive section at PITZ", DIPAC2009.

ISBN 978-3-95450-126-7